



Bacteriology | Full-Length Text

The histidine kinase NahK regulates pyocyanin production through the PQS system

Alicia G. Mendoza,¹ Danielle Guercio,² Marina K. Smiley,³ Gaurav K. Sharma,⁴ Jason M. Withorn,⁴ Natalie V. Hudson-Smith,⁴ Chika Ndukwe,⁴ Lars E. P. Dietrich,³ Elizabeth M. Boon⁴

AUTHOR AFFILIATIONS See affiliation list on p. 15.

ABSTRACT Many bacterial histidine kinases work in two-component systems that combine into larger multi-kinase networks. NahK is one of the kinases in the GacS Multi-Kinase Network (MKN), which is the MKN that controls biofilm regulation in the opportunistic pathogen *Pseudomonas aeruginosa*. This network has also been associated with regulating many virulence factors *P. aeruginosa* secretes to cause disease. However, the individual role of each kinase is unknown. In this study, we identify NahK as a novel regulator of the phenazine pyocyanin (PYO). Deletion of *nahK* leads to a fourfold increase in PYO production, almost exclusively through upregulation of phenazine operon two (*phz2*). We determined that this upregulation is due to mis-regulation of all *P. aeruginosa* quorum-sensing (QS) systems, with a large upregulation of the *Pseudomonas* quinolone signal system and a decrease in production of the acyl-homoserine lactone-producing system, *las*. In addition, we see differences in expression of quorum-sensing inhibitor proteins that align with these changes. Together, these data contribute to understanding how the GacS MKN modulates QS and virulence and suggest a mechanism for cell density-independent regulation of quorum sensing.

IMPORTANCE *Pseudomonas aeruginosa* is a Gram-negative bacterium that establishes biofilms as part of its pathogenicity. *P. aeruginosa* infections are associated with nosocomial infections. As the prevalence of multi-drug-resistant *P. aeruginosa* increases, it is essential to understand underlying virulence molecular mechanisms. Histidine kinase NahK is one of several kinases in *P. aeruginosa* implicated in biofilm formation and dispersal. Previous work has shown that the nitric oxide sensor, NosP, triggers biofilm dispersal by inhibiting NahK. The data presented here demonstrate that NahK plays additional important roles in the *P. aeruginosa* lifestyle, including regulating bacterial communication mechanisms such as quorum sensing. These effects have larger implications in infection as they affect toxin production and virulence.

KEYWORDS nitric oxide, NosP, NahK, pyocyanin, PQS, quorum sensing, signaling, virulence

Pseudomonas aeruginosa is a Gram-negative bacterium that establishes biofilms as part of its pathogenicity. P. aeruginosa is associated with nosocomial infections that cause complications for patients with cystic fibrosis, cancer, or burn wounds (1). The most at-risk patient groups are those on ventilators, a problem intensified by increased ventilator use during the SARS-CoV-2 (severe acute respiratory syndrome coronavirus 2) pandemic (2). Acute P. aeruginosa infections that lead to sepsis are typically associated with the planktonic state, where the bacteria travel around the body infecting various organs rapidly (1, 3). Chronic P. aeruginosa infections can lead to pulmonary illnesses, especially in people who already have higher susceptibility to respiratory problems, such as cystic fibrosis patients (4). These chronic infections are usually associated with the

Editor Joseph Bondy-Denomy, University of California San Francisco, San Francisco, California, USA

Address correspondence to Elizabeth M. Boon, elizabeth.boon@stonybrook.edu.

The authors declare no conflict of interest.

See the funding table on p. 15.

Received 21 August 2023 Accepted 12 December 2023 Published 3 January 2024

Copyright © 2024 American Society for Microbiology. All Rights Reserved.

biofilm or sessile state (1, 4). This planktonic-to-sessile switch is an essential part of *P. aeruginosa* virulence.

The GacS Multi-Kinase Network (MKN) regulates the planktonic-to-sessile switch (3, 5). Several kinases, including GacS, PA1611 (PA14_43670), RetS, SagS, and NahK, signal in this network to regulate the activity of a post-transcriptional global regulator protein, RsmA (Fig. 1A) (3, 5). RsmA inhibits translation of mRNAs related to biofilm formation, quorum sensing (QS), pyocyanin (PYO) production, and type VI secretion systems, promoting the planktonic state (3, 5). RsmA is inactivated by the small regulatory RNAs, rsmY and rsmZ, which are transcribed in response to MKN activity (3, 5). All kinases in this network are hybrid histidine kinases that respond to extracellular signals which include nitric oxide (NO), glycan mucins, and calcium ions. However, further study is needed to identify additional signals and determine the physiological consequences for how these signals modulate RsmA activity (5–8).

NO is a diatomic gas that signals biofilm dispersal in many bacteria at low nanomolar to picomolar concentrations (10). The source of NO to which P. aeruginosa has evolved this response is unknown. It could be host-derived, environmental, or derived from P. aeruginosa denitrification. In P. aeruginosa, the NO-sensing protein NosP is necessary for biofilm dispersal (6). At a molecular level, NosP functions by inhibiting its cocistronicassociated kinase, NahK, when in the ferrous NO-ligated state (6). NahK is one of four kinases that regulate the phosphorylation state of HptB, which is one of the main response regulators in the GacS MKN (6, 11). When HptB is not phosphorylated, HptB indirectly activates transcription of rsmY, leading to inactivation of RsmA and, thus, promotes biofilm formation (5). NosP and NahK have also been identified as part of the Pseudomonas biofilm transcriptome through comparative transcriptome analysis of 138 biofilm-forming clinical *Pseudomonas aeruginosa* isolates (12). Outside of these works, not much is known about the molecular roles of NosP and NahK in biofilm regulation and other cellular processes, even though the GacS MKN is implicated in essential bacterial processes including QS, antibiotic resistance, metabolism, replication, and virulence (3, 12, 13).

In *P. aeruginosa*, three QS systems act sequentially: *las*, *rhl*, and *pqs* (13). RsmA and the GacS MKN control QS and phenazine production as part of their global regulon (5). When RsmA is active, it inhibits translation of *lasR* and *rhlR* (13). At high cell density, RsmA repression is relieved, allowing for QS to occur, which also results in phenazine production (13). PYO production is controlled, in part, by all three QS systems that contribute to the transcriptional activation of two phenazine-producing operons, *phzA1-G1* (*phz1*) and *phzA2-G2* (*phz2*) (14). These operons are ~98% identical at the genomic level and each one is sufficient to confer production of phenazine-1-carboxylic acid (PCA), a precursor to the well-characterized blue phenazine, PYO. LasR and RhlR are known to activate *phz1* directly, while the *Pseudomonas* quinolone signal (PQS) influence on *phz2* is indirect through an unknown mediator (15). These operons are also controlled by additional factors, such as other transcription factors and QS inhibitor proteins (13, 16). While both operons contribute to phenazine production, *phz2* is more important than *phz1* for host colonization in mouse models (14).

Many factors in the GacS MKN have been shown to influence PYO production (5, 8, 17, 18). Deletion of hptB leads to decreases in motility and virulence, but effects on PYO or other toxins were not reported (11, 19). gacS and gacA deletions have shown decreases in virulence and biofilm production, with some reports showing a twofold decrease in PYO production (8, 18, 20). In P, aeruginosa strain PAO1, $\Delta rsmY$ and $\Delta rsmZ$ have been shown to have decreases in PYO production, while $\Delta rsmA$ has a modest increase in PYO levels, about twofold compared to wild type (18). Recently, $\Delta retS$ in P, aeruginosa strain PAO1 has been shown to also have an increase in PYO production similar to $\Delta rsmA$, with an increase of about twofold (8). Overall, this suggests a novel regulation of PYO by NahK in this network. Here, we describe a novel role for NahK in modulation of the PQS system, which results in downregulation of phz2 expression, and, therefore, also decreases PYO production.

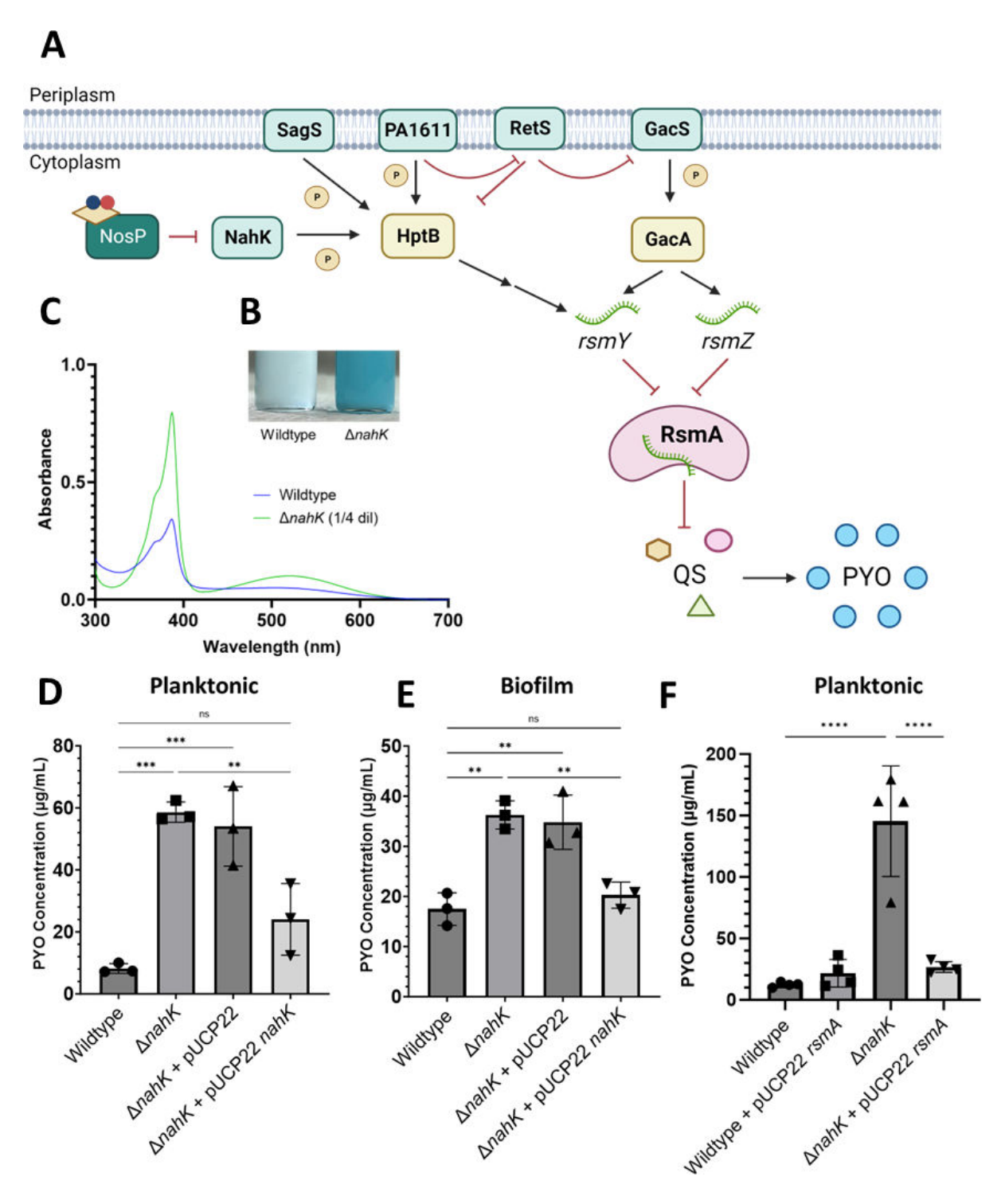


FIG 1 Pyocyanin is overproduced in $\Delta nahK$. (A) Representation of NahK in the GacS MKN. All kinases function to regulate the activity of post-transcriptional regulator protein, RsmA. RsmA activity regulates quorum sensing, which in turn regulates PYO production. (B) Chloroform extract of $\Delta nahK$ supernatant has a bright blue color. (C) PYO is characterized by a peak at 520 nm in 0.1M HCl (9). $\Delta nahK$ is diluted fourfold in 0.1M HCl compared to wild type. (D, E) Beer's law quantification of pyocyanin production at 520 nm (extinction coefficient 17.072 from 21). (D) Planktonic, liquid cultures (n = 3), and (E) biofilm, agar cultures. n = 3. (F) Overexpression of rsmA in wild type and $\Delta nahK$ complements the PYO phenotype, suggesting that absence of rsmA in wild type and rsmA activity, which in turn increases PYO production. rsmA represses RsmA activity, which in turn increases PYO production. rsmA represses the calculated using one-way analysis of variance and a Tukey multiple comparisons test. rsmA in the calculated using one-way analysis of variance and a Tukey multiple comparisons test. rsmA in the calculated using one-way analysis of variance and a Tukey multiple comparisons test.

RESULTS

Deletion of nahK leads to overproduction of the phenazine PYO

After discovering the role of NosP and NahK in biofilm dispersal, we became interested in how these proteins individually contribute to RsmA-dependent phenotypes (Fig. 1A) (6). We generated a genetic deletion of nahK and found that this strain secreted a blue pigment into the culture supernatant (Fig. 1B). The blue coloration indicated the phenazine PYO, which we verified using acidified-chloroform extraction of supernatant and UV-visible light spectroscopy (Fig. 1C) (9). The $\Delta nahK$ strain showed a fourfold increase of PYO in planktonic culture and a twofold increase in biofilms relative to wild type (Fig. 1D and E) (21). PYO production was reduced by complementation of nahK in both planktonic and biofilm cultures (Fig. 1D and E). Finally, we determined that the $\Delta nahK$ strain regulates PYO production through RsmA by overexpressing rsmA in $\Delta nahK$ on a constitutively active promoter. The $\Delta nahK rsmA$ overexpression strain shows complete complementation of the $\Delta nahK$ PYO phenotype (Fig. 1F). This result indicates that RsmA is inactive in $\Delta nahK$, leading to the PYO production increase.

ΔnahK is more virulent than PA14 wild type

PYO is a redox-active pigment that contributes to P. aeruginosa pathogenicity by generating reactive oxygen species. For example, PYO has been shown to result in death of neutrophils by interfering with their mitochondrial respiratory chain (22). To determine if $\Delta nahK$ is more virulent than wild type P. aeruginosa PA14, we performed a Caenorhabditis elegans slow-killing assay. Over 4 days, only 36% of worms survived that were fed with $\Delta nahK$, compared to 78% survival of worms fed with wild type (Fig. 2). This reduction was partially restored by complementing the $\Delta nahK$ strain with nahK expressed off a plasmid (Fig. 2). We have additionally shown a similar phenotype in a mung bean virulence model that demonstrates $\Delta nahK$ kills sprouts more readily than wild type (Fig. S1).

ΔnahK mis-regulates phenazine biosynthesis genes

We then set to determine the molecular mechanism of NahK-dependent regulation of PYO production. Phenazine biosynthesis occurs through a branched, multi-step pathway (23). The first step is the conversion of chorismic acid to PCA by the two redundant phenazine operons, *phz1* and *phz2*, which have ~98% DNA sequence homology (14, 15, 23). Despite their conservation, the two operons are under the control of different promoter sequences, leading to differential regulation (14, 15). In PA14, both *phz1* and *phz2* contribute to phenazine production in planktonic cultures while, during biofilm growth, *phz2* is the dominant operon (14). Therefore, we investigated which *phz* operon was responsible for NahK-dependent PYO production in planktonic culture.

To study the transcriptional activity of each operon, we generated mScarlet transcriptional reporters with the promoters of phz1 or phz2 driving mScarlet expression and genomically integrated them into wild type and $\Delta nahK$ strains. We then grew the strain planktonically for 24 h and tracked the mScarlet fluorescence signal (Fig. 3A). We found that expression of the Pphz2-mScarlet reporter was increased in both strains compared to Pphz1-mScarlet. Pphz1-mScarlet had minimal expression in both wild type and $\Delta nahK$ (Fig. 3A). $\Delta nahK$ att8::Pphz2-mScarlet had higher expression than the wild type, suggesting that phz2 was upregulated in $\Delta nahK$, giving rise to the PYO overproduction phenotype (Fig. 3A and 1D). This same trend was also observed in biofilm; however, the differences were not statistically significant (Fig. 3B). This trend is expected since phenazine production in biofilms is mostly phz2-dependent (14). As with PYO overproduction (Fig. 1F), this phenotype is also complemented by overexpression of rsmA in $\Delta nahK$ attB::Pphz2-mScarlet (Fig. S2), indicating that a lack of nahK results in a loss of rsmA, which is consistent with NahK acting through the GacS MKN and RsmA to regulate the phz2 operon.

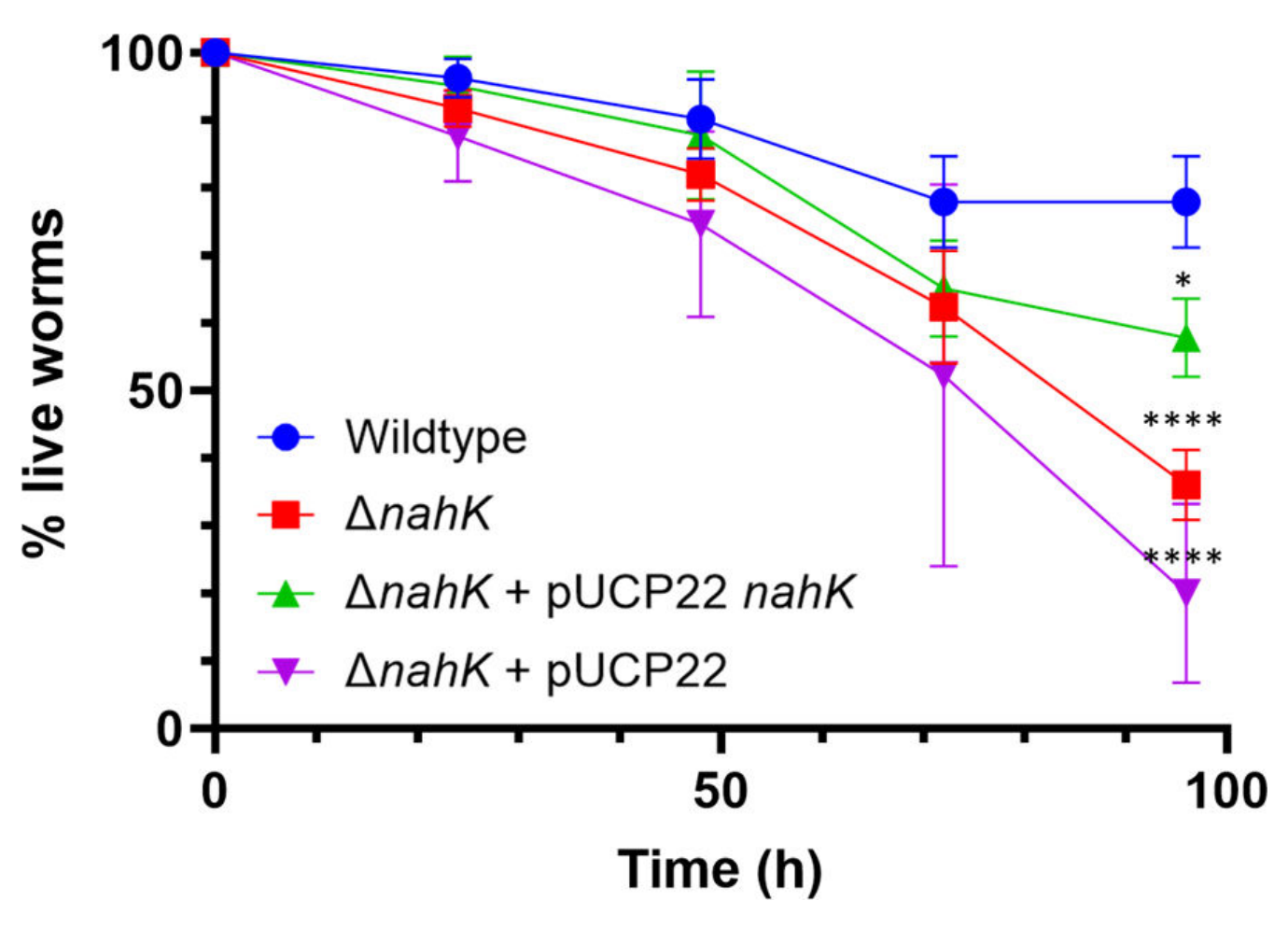


FIG 2 \triangle *AnahK* is more virulent than PA14 wild type. Slow-killing kinetics of all strains in the nematode *C. elegans*. After 5 days of exposure to the bacteria, wild type shows ~20% killing, while \triangle nahK shows ~55% killing. Error bars represent the standard deviation of at least four biological replicates, with each replicate consisting of 30–35 worms. *P*-values were calculated using one-way analysis of variance. * $P \le 0.5$, **** $P \le 0.0001$.

The conversion of PCA to PYO is mediated by two enzymes: the S-adenosyl methionine (SAM)-dependent methyltransferase PhzM converts PCA to 5-methylphenazine-1-carboxylic acid betaine (23, 24). The oxygen-dependent monooxygenase PhzS converts 5-methylphenazine-1-carboxylic acid betaine to PYO (25–27). PhzS can also use PCA as a substrate to make 1-hydroxyphenazine (23, 28, 29). To further determine that phz2 drives PYO production in $\Delta nahK$, we generated $\Delta nahK$ strains that contained deletions of either phz1 or phz2 and quantified phenazine production. These strains were also $\Delta phzH\Delta phzM\Delta phzS$ (ΔHMS); therefore, the only phenazine produced is PCA. When phenazines were quantified, $\Delta nahK\Delta phz1HMS$ produced PCA levels comparable to $\Delta nahK$ (Fig. 3C). $\Delta nahK\Delta phz2HMS$ generated nearly no detectable PCA, suggesting that nearly all phenazines produced by $\Delta nahK$ are produced by phz2 (Fig. 3C).

To assess if PhzM and PhzS are affected by NahK, we assessed the expression of these corresponding genes in $\Delta nahK$ (Fig. 3D). Indeed, both *phzM* and *phzS* were upregulated in $\Delta nahK$ compared to wild type (Fig. 3D).

Quorum sensing is mis-regulated in ΔnahK

Both *phz* operons, *phzM* and *phzS*, are regulated by QS (15). To understand how QS systems are involved in modulating PYO production in our system, we performed quantitative PCR (qPCR) on the regulators of the *phz* operons (Fig. 4). *Phz1* is activated by two of the main QS pathways, the *las* and *rhl* systems (13). Lasl and RhII are lactone synthases that make N-acyl homoserine lactones, which activate the transcription factors

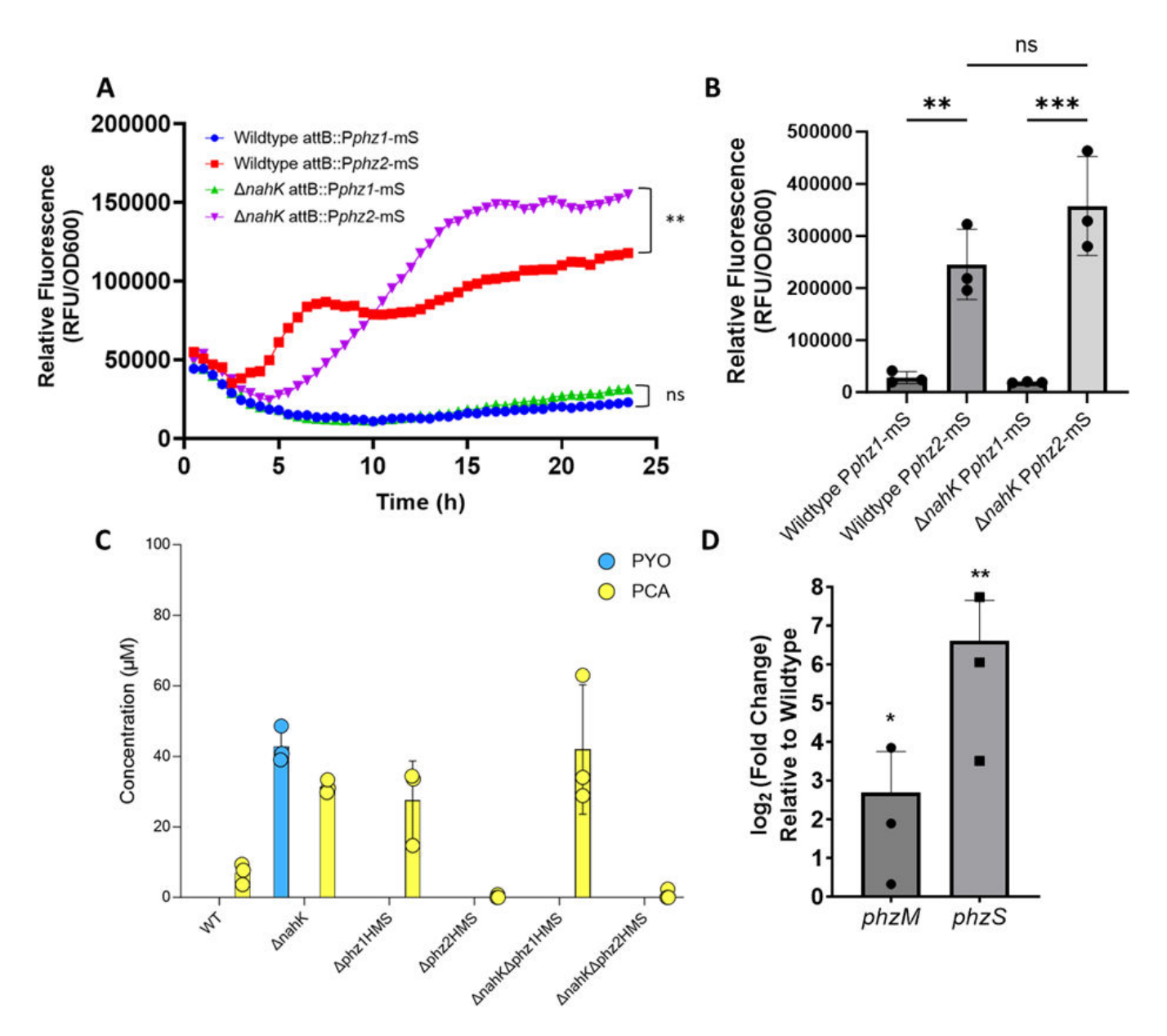


FIG 3 *Phz2* is the driver of PYO production. (A) *Pphz2*-mS is expressed more than *Pphz1*-mS in the wild type and Δ*nahK* planktonically. Δ*nahK* has higher expression of *Pphz2*-mS than wild type overall. *P*-values were calculated using one-way analysis of variance and a Tukey multiple comparisons test at final time point. n = 3. (B) *Pphz2*-mS is expressed more than *Pphz1*-mS in the wild type and Δ*nahK* biofilms. *P*-values were calculated using one-way analysis of variance and a Tukey multiple comparisons test. n = 3. (C) High-performance liquid chromatography (HPLC) quantification of phenazines PCA and PYO in wild type, Δ*nahK*, Δ*nahKΔphz1HMS*, and Δ*nahKΔphz2HMS*. n = 3. (D) Quantitative PCR for *phzM* and *phz5* in Δ*nahK* compared to wild type. Gyrase A was used as a housekeeping gene (30,). *P*-values were calculated using unpaired, two-tailed *t*-tests comparing Δ*nahK* ΔCt values to wild type ΔCt values. n = 3. **P*-value <0.05, ***P*-value <0.01, *** *P*-value <0.001.

LasR and RhIR (15, 30, 31). In agreement with Fig. 3, factors that activate phz1 showed no difference in transcriptional levels in $\Delta nahK$ compared to wild type levels (Fig. 4). phzM and phzS are also thought to be controlled primarily through the las and rhI systems because these genes flank the phz1 operon. This may suggest a role for the las and rhI systems in the $\Delta nahK$ phenazine phenotype that is not appreciated by the fluorescent transcriptional reporter.

Regulation of *phz2* is not mediated by LasR/RhIR directly and is overall not as well understood as that for *phz1* (14, 15). *phz2* is activated primarily by two factors: QS inhibitor protein RsaL and PQS (14). RsaL is a global transcription factor that can be

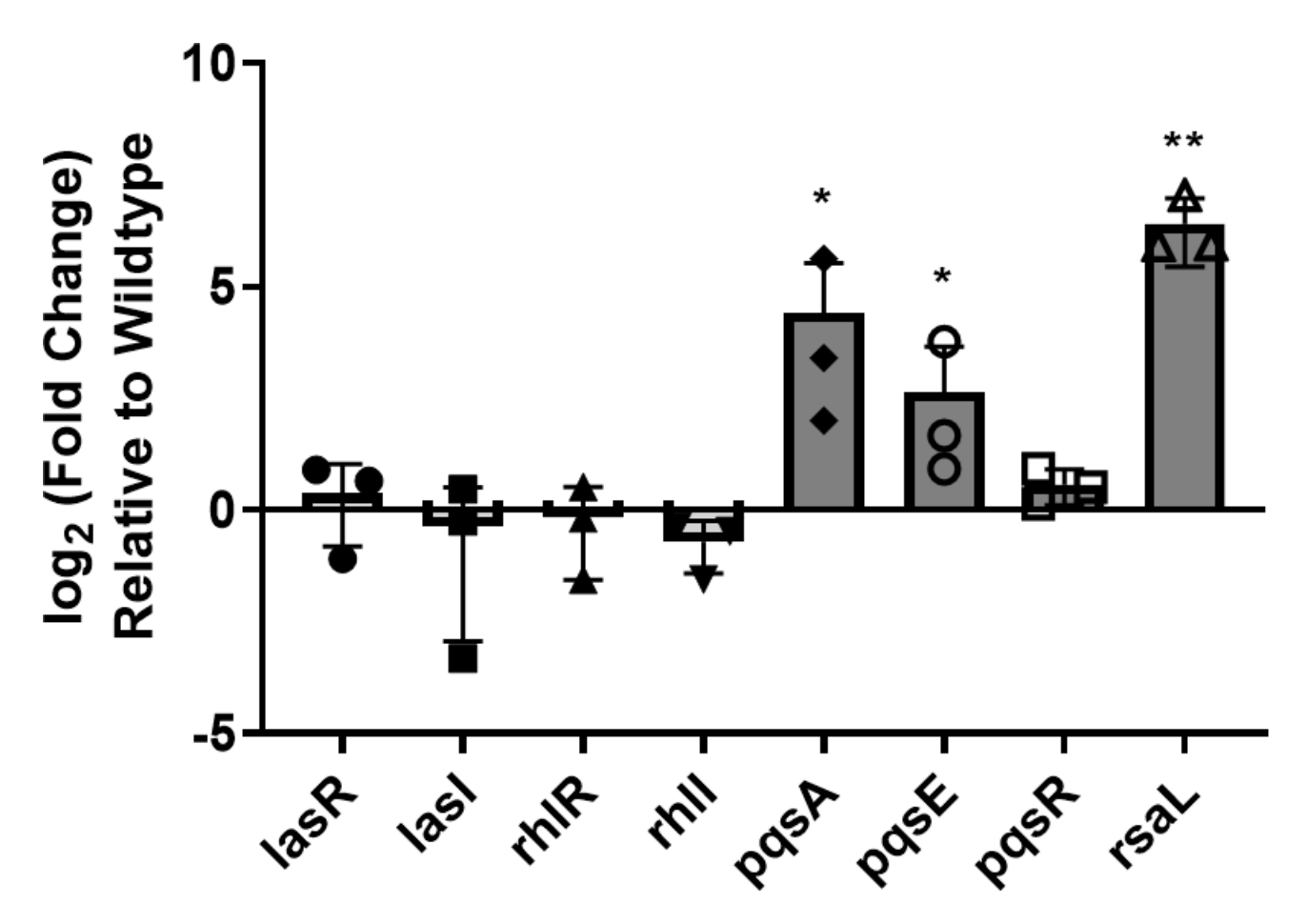


FIG 4 Pyocyanin production may be regulated by the PQS system and *rsal*. qPCR for the main quorum-sensing transcriptional regulators in Δ*nahK* compared to wild type. Pyocyanin production is potentially induced by each of these transcriptional regulators. Gyrase A was used as a housekeeping gene (30). Bars above and below the threshold represent upregulation and downregulation, respectively. *P*-values were calculated using unpaired, two-tailed *t*-tests comparing Δ nahK Δ Ct values to wild type Δ Ct values. n = 3. **P*-value <0.05, ***P*-value <0.01.

activated by LasRI and is involved mostly in combating oxidative stress (15). It is also mostly studied within the context of the *las* system, as RsaL represses the *las* operon (32). It is believed that RsaL indirectly controls *phz2* via an unidentified regulator (15).

PQS is a QS molecule that has additional functions of iron binding and antioxidant properties (33). phz2 expression correlates directly with PQS production; when PQS is upregulated, phz2-mediated PCA production is upregulated (15). PQS is also synthesized from precursor molecule chorismic acid and converted to PQS by the pqs operon which includes pqsABCD and pqsE (33, 34). Current research suggests pqsE can be differentially regulated in the absence of RhIR and compensate for some RhIR-mediated transcriptional regulation (35). MvfR/PqsR senses PQS and regulates the pqs operon (13). Genes in the pqs operon and rsaL are highly upregulated in $\Delta nahK$ compared to wild type (Fig. 4).

To corroborate these results, we performed untargeted liquid chromatography–mass spectrometry (LCMS) to quantify QS molecules from the bacterial supernatant of the wild type and $\Delta nahK$ strains (Fig. 5; Fig. S3). PYO and PYO precursors, including PCA and phenazine-1,6-dicarboxylic acid (PDC), were more present in $\Delta nahK$ supernatant compared to wild type. PQS derivatives, like 2-heptyl-4-quinolone (HHQ) and dihydroxy-quinoline (DHQ), were more prevalent in $\Delta nahK$ compared to wild type (Fig. 5). Interestingly, we found a reduction in N-(3-oxododecanoyl)-L-homoserine lactone (C12-HSL) production in $\Delta nahK$, suggesting that there may be post-transcriptional regulation of the *las* quorum-sensing system. Many pathogenic and clinically relevant strains of *Pseudomonas aeruginosa* have defects or deletions in the *las* system (36). This may relate to other

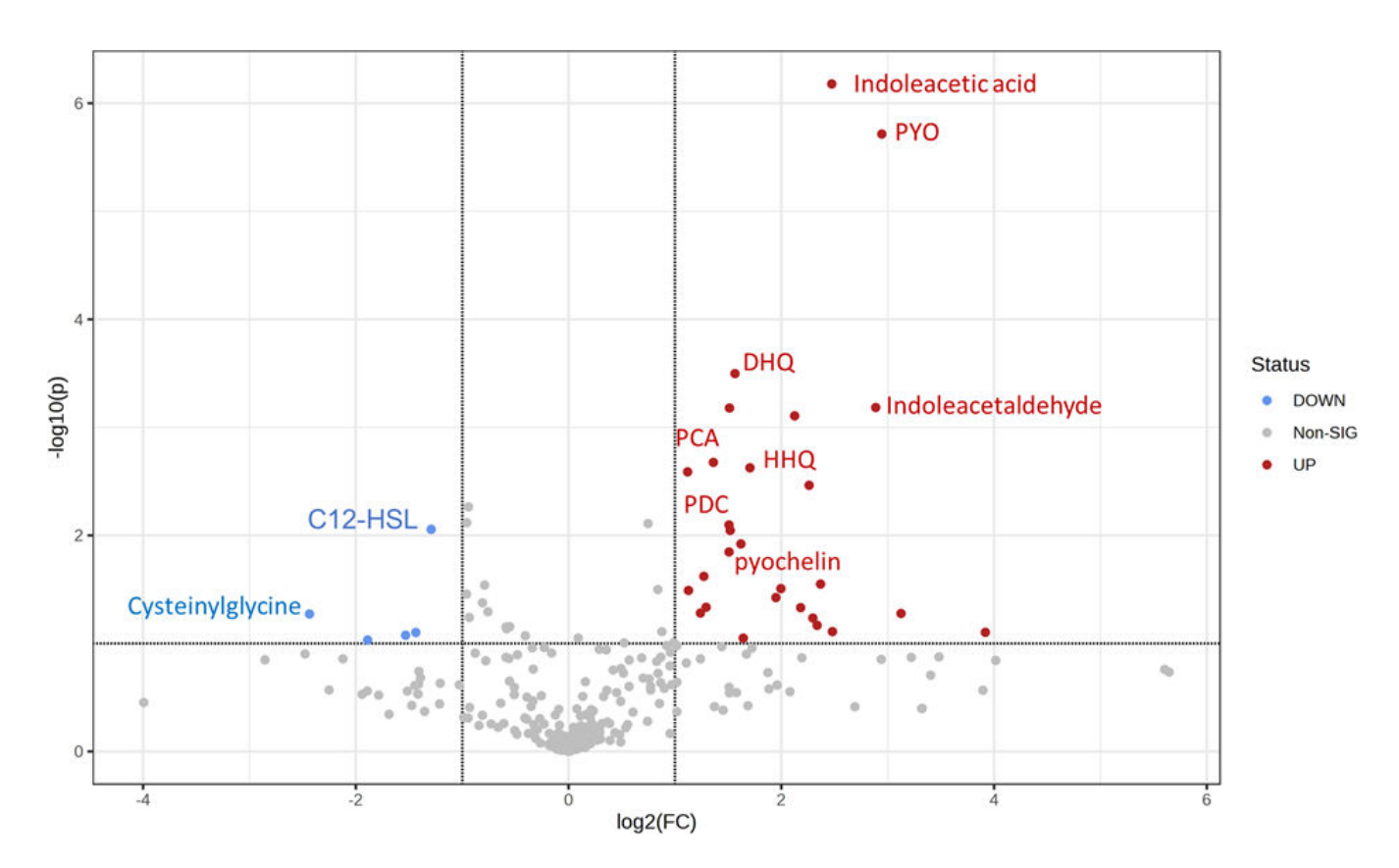


FIG 5 PQS precursors are overexpressed in $\triangle nahK$ supernatant, while C12-HSL is reduced. Values are a ratio of prevalence in $\triangle nahK$:wild type in positive mode LCMS. Bars above and below the threshold represent upregulation and downregulation, respectively. P-values were calculated using unpaired, two-tailed t-tests (Table S4).

ways ΔnahK is more virulent than wild type, possibly separate from PYO production (Fig. 2). RsmA activity is also known to inhibit the Las system post-transcriptionally, which overall promotes pathogenicity (37). Because NahK activity may regulate RsmA activity through the HptB branch of the GacS MKN, this may suggest that deletion of nahK improperly promotes RsmA activity, leading to these changes in QS.

Quorum sensing is mis-regulated at both a transcriptional and post-translational level

QS systems in P. aeruginosa have several layers of regulation. First, these systems work sequentially as a function of cell density and regulate each other (the las system activates the rhl system, which in turn inactivates las). A similar feedback mechanism has been described for rhl and pqs, where RhIR activates the pqs operon and PqsR turns off the rhl operon (13). QS is also regulated by QS inhibitor proteins, many of which need further characterization (13). The best-characterized inhibitors include RsaL and QscR, inhibitors of the las system, QteE, inhibitor of the rhl system, and QsIA, inhibitor of the pqs system (38–40). The mechanism of inhibition is typically by protein-protein interaction, where the inhibitor binds the transcription factor, inactivating it (13). Because these are protein-protein interactions, we hypothesized that if inhibition of the las and rhl system was occurring, this inhibition would not be seen in the transcription levels of the transcription factors LasR and RhIR via qPCR (Fig. 4). Using qPCR, we examined relative levels of each inhibitor in $\Delta nahK$ compared to wild type (Fig. 6). As expected, we saw an increase in QS inhibitors for the las and rhl systems, and a decrease in the inhibitor for the pqs system (Fig. 4 and 6).

Surprisingly, overexpression of QS inhibitors in wild type or $\Delta nahK$ does not appear to affect PYO production (Fig. S4). Overexpression of rsaL or qslA does not change PYO

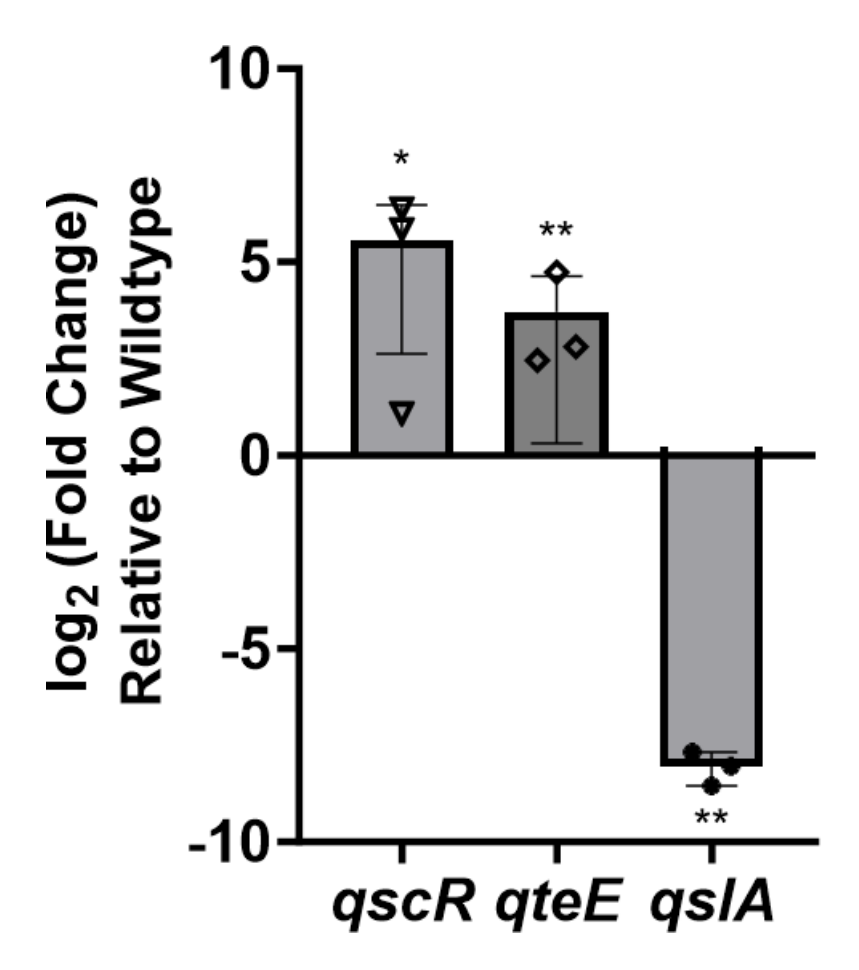


FIG 6 Quorum-sensing inhibitors for the *las* and *rhl* systems are upregulated, whereas the *pqs* inhibitor is downregulated. qPCR for the main QS inhibitors in $\Delta nahK$ compared to wild type. Gyrase A was used as a housekeeping gene. Bars above and below the threshold represent upregulation and downregulation, respectively. *P*-values were calculated using unpaired, two-tailed *t*-tests comparing $\Delta nahK$ Δ Ct values to wild type Δ Ct values. n = 3. **P*-value <0.05, ***P*-value <0.01.

production in PA14 wild type (Fig. S4A). Overexpression of qslA in $\Delta nahK$ does not complement the PYO overexpression phenotype (Fig. S4B). Several qslA-regulating factors have been suggested, including PA0225, PA2758, PA1315, PA0479, and CatR (41). In $\Delta nahK$ relative to wild type, unlike qslA, these genes are not differentially regulated; the only gene with a slight downregulation is PA0479 (Fig. S5A). In a $\Delta nahK + pUCP22$ rsmA ($\Delta nahK rsmA++$) strain compared to wild type, the expression of these genes was also unchanged compared to wild type (Fig. S5B). Therefore, these qslA-regulating factors appear to be independent of the NahK and the GacS MKN. It is likely that the GacS MKN is an additional qslA regulating system.

PQS promotes phz2 expression in Δ nahK

Once we found that PQS was increased in $\Delta nahK$, we then asked if PQS was increasing phz2-mediated PYO production in our strains. To determine this, we devised a co-culture experiment. A donor strain, either wild type or $\Delta nahK$, would provide PQS to a recipient strain that could not produce PQS ($\Delta pqsABC$) but did encode for either the phz1 or phz2 transcriptional mScarlet reporter ($\Delta pqsABC$ attB::Pphz1-mS and $\Delta pqsABC$ attB::Pphz2-mS). Upon co-culturing, we could track activation of the phz reporters as a function of growth. Wild type or $\Delta nahK$ would provide PQS that activates phz2 in $\Delta pqsABC$ attB::Pphz2-mS in a manner dependent on amount of PQS secreted. $\Delta pqsABC$ attB::Pphz-mS reporter strains did not activate the reporters during their own growth, only when co-cultured (Fig. S6).

When co-cultured with wild type, phz2 activated more than phz1, similar to our previous finding in Fig. 4 (Fig. 7A). When co-cultured with $\Delta nahK$, phz2 activated more than phz1, and phz2 activation was increased compared to wild type phz2 activation levels (Fig. 7A). To further confirm this was due to PQS itself, we also generated $\Delta pqsR$ attB::Pphz reporter recipient strains that are unable to respond to PQS. These strains, when co-cultured with either wild type or $\Delta nahK$, showed no activation of either reporter (Fig. S6A). In

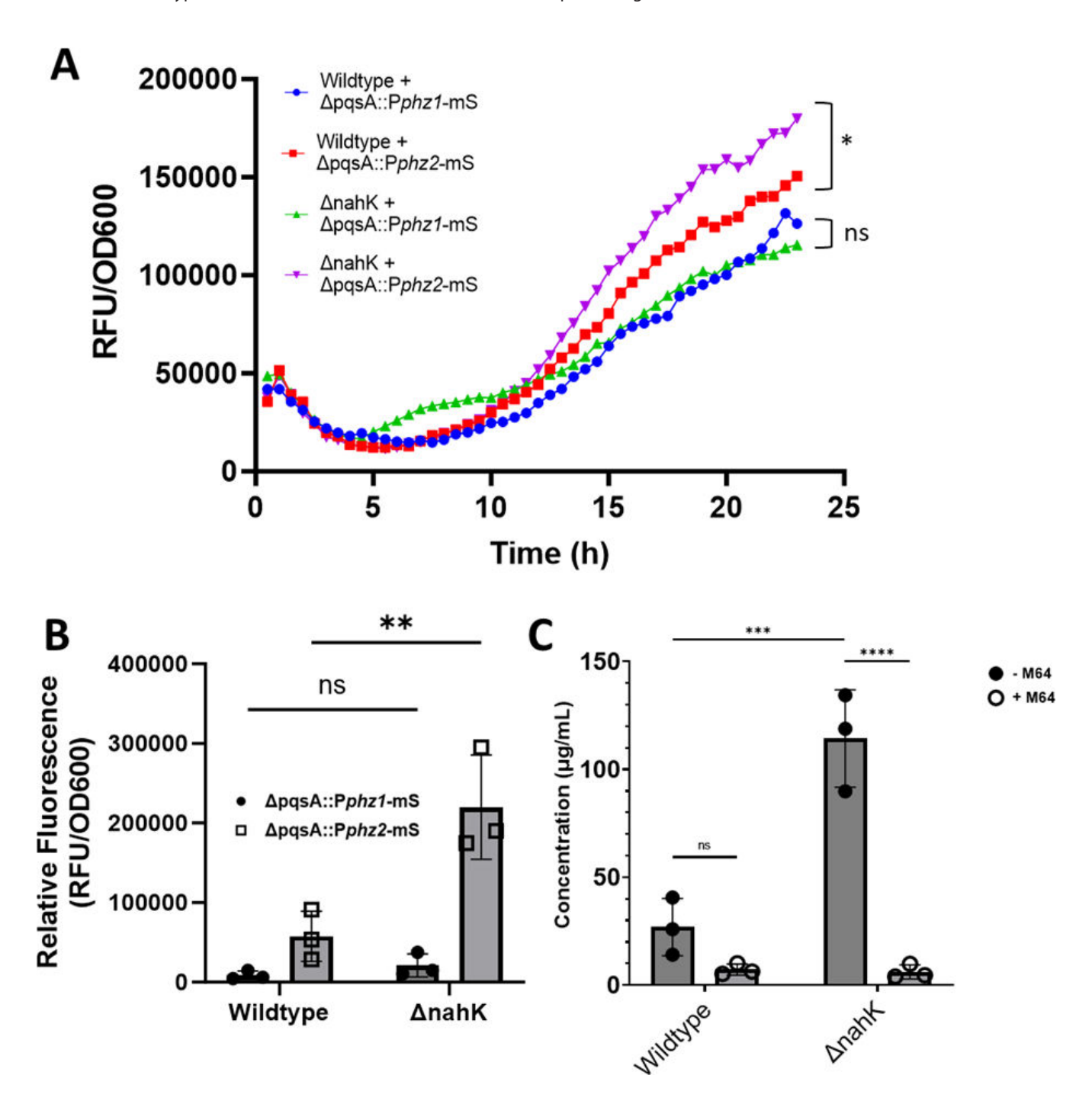


FIG 7 PQS drives phz2 in ΔnahK. (A) Co-cultured wild type or ΔnahK with ΔpqsABC (planktonic) containing either the phz1 or phz2 mScarlet reporter shows increased activation of phz2 with both donors, with a higher activation in ΔnahK. n=3. P-values were calculated using one-way analysis of variance and a Tukey multiple comparisons test at final time point. * $P \le 0.05$. (B) 3-day biofilms of co-cultured wild type or ΔnahK with ΔpqsABC containing either the phz1 or phz2 mScarlet reporter show increased activation of phz2 with both donors, with a higher activation in ΔnahK. n=3. P-values were calculated using one-way analysis of variance and a Tukey multiple comparisons test at final time point. * $P \le 0.05$.

January 2024 Volume 206 Issue 1 10.1128/jb.00276-23**10**

addition, co-cultured wild type or $\Delta nahK$ with $\Delta pqsABC$ attB::Pphz2-mS showed increased activation in a 3-day colony biofilm (Fig. 7B).

We then determined PYO concentrations in wild type and $\Delta nahK$ supernatants after exposure to 1 μ M of the PqsR inhibitor, M64 (42). With M64, both wild type and $\Delta nahK$ had diminished PYO production, further suggesting PQS was driving PYO production (Fig. 7C). Overall, this suggests that $\Delta nahK$ overexpresses phz2-mediated PYO because the strain generates an increased amount of PQS.

DISCUSSION

Here, we describe the effect of the histidine kinase (HK) NahK on the PQS-dependent production of the phenazine PYO in *P. aeruginosa* PA14 (Fig. 8). NahK is conserved in many Gram-negative bacteria, and NO regulation of QS systems has been studied in *Vibrio cholerae, Vibrio harveyi*, and *Staphylococcus aureus* (43–45). In *V. cholerae*, the *nosP/nahK* operon encodes for *Vc*NosP, a NO sensor, and hybrid HK VpsS. The mechanism is similar; NO-bound NosP (VpsV) inhibits VpsS, leading to dispersal. There, VpsS affects QS by transferring a phosphoryl group to LuxU, and subsequently to the transcription factor

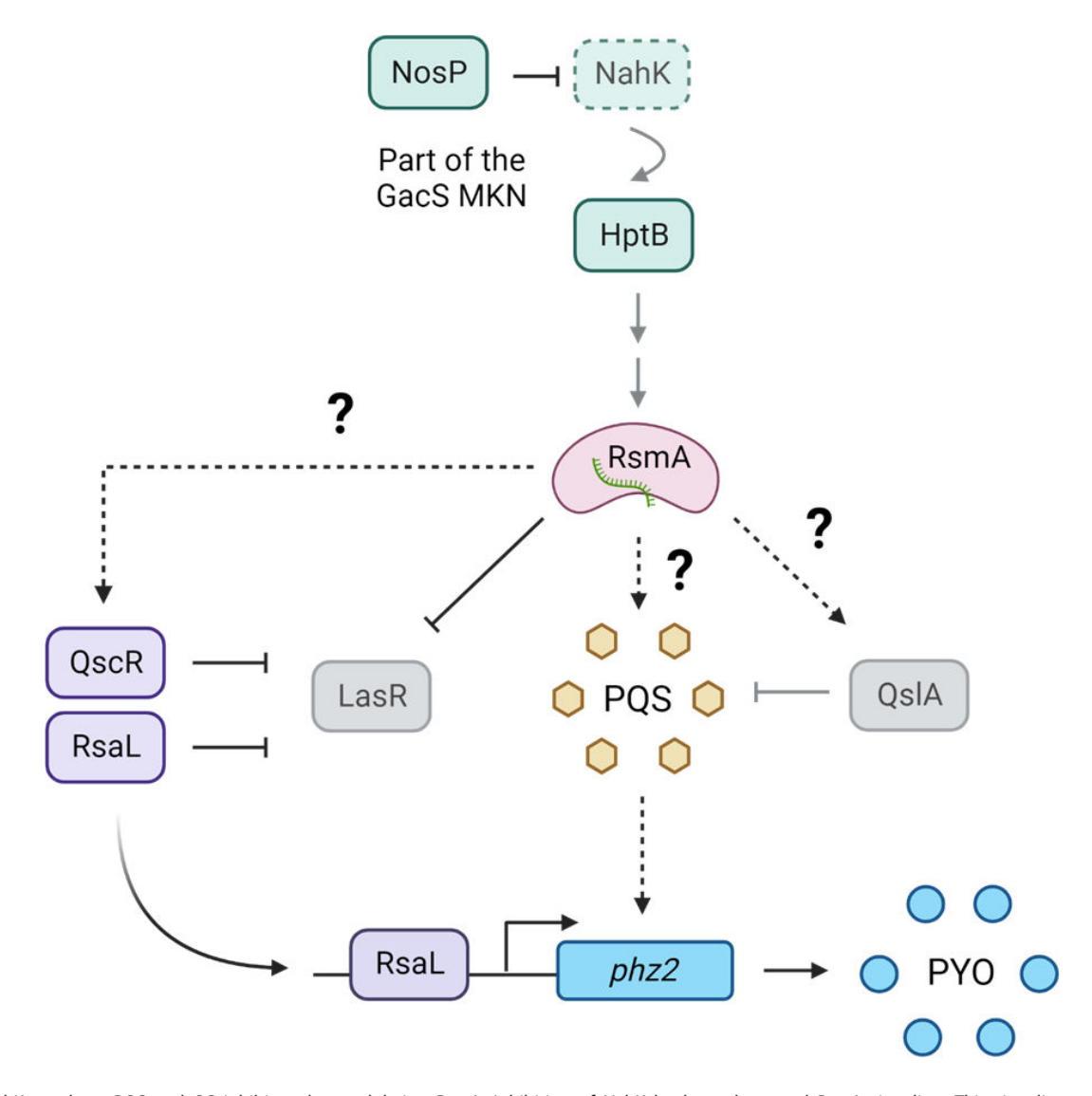


FIG 8 NahK regulates PQS and QS inhibitors by modulating RsmA. Inhibition of NahK leads to decreased RsmA signaling. This signaling activates PQS production and represses PQS inhibitor QslA. It also represses the LasR system through activation of LasR QS inhibitors. Increased RsaL and PQS production increases phz2-mediated PYO production.

LuxO, which results in increased virulence and biofilm formation at low cell density (43). Therefore, it was reasonable to hypothesize that in *P. aeruginosa*, the *nosP/nahK* operon would influence QS and its downstream effectors. However, it is surprising how large of an effect $\Delta nahK$ has on PYO production that was previously unexplored.

The GacS MKN that NahK is implicated in has been shown to indirectly affect PYO production through RsmA regulation of QS (3, 5). In PAO1, $\Delta rsmY$ and $\Delta rsmZ$ have been shown to decrease PYO, while $\Delta rsmA$, $\Delta gacS$, and $\Delta retS$ have shown increases in PYO (8, 18, 46). Many studies focus on how these GacS MKN factors influence the Las and Rhl systems, suggesting these modulations of PYO are potentially through a phz1-mediated overexpression, rather than a phz2-mediated one (5). Our data instead suggest these changes in PYO may be the result of changes in PQS production and phz2 expression. However, deletions of all factors in the GacS MKN need to be characterized more robustly in PA14 to establish this mechanism.

The data presented here could also suggest that there is a more direct link between NahK and QS. It is possible that NahK can either heterodimerize with other kinases in *P. aeruginosa* or phosphorylate other proteins. Recently, these types of interactions have been appreciated for other kinases in the GacS MKN. Orphan sensor kinase SagS is known to crosstalk outside of the GacS MKN with BfiS and NicD to regulate cyclic di-GMP and *rsmZ* levels, both to control biofilm formation in a Gac-independent manner (17). In *Shewanella oneidensis*, *So*NahK is known to phosphorelay with three response regulators, leading to transcriptional and cyclic di-GMP production changes (47). Based on what is known in *S. oneidensis* and other kinases in the *P. aeruginosa* GacS MKN, it is possible that NahK could have another unidentified response regulator. This requires additional research.

It is also surprising that *nahK* has not appeared in screens for regulators of PYO. It has been suggested that the *nosP/nahK* operon is QS-regulated (12, 48). Letizia et al. suggest that, in the absence of all other QS transcription factors and signaling molecules, RhIR downregulates the *nosP/nahK* operon in PAO1 (48). Perhaps, NahK functions as an important intermediate to transition from the Las/RhI systems to the PQS system during stationary phase. There may be a mechanism where RhIR transcriptionally represses NahK to lower NahK signaling, which would therefore activate the PQS system, similar to how deletion of *nahK* promotes PQS production as shown here. However, additional research is required to know when NosP and NahK are present and active in the bacteria.

NahK may also play an important role in connecting PYO, biofilm regulation, and anaerobic respiration. Intracellular NO levels in *P. aeruginosa* are indirectly regulated by all three QS systems because they play a role in controlling the denitrification machinery (49). PQS specifically regulates denitrification processes, so there is potential for a feedback loop between NosP/NahK signaling, PQS production, and NO produced by the denitrification process and/or anaerobic respiration. While PQS is not usually present microaerobically (PQS is generated from HHQ by PqsH, which is a flavin adenine dinucleotide [FAD]-dependent monooxygenase) many of the precursors are produced anaerobically (33).

For example, HHQ is produced by several enzymes (PqsABCDE) from anthranilic acid. HHQ can bind most substrates PQS can bind with $100\times$ less avidity (33). Therefore, in large excess, as seen in the $\Delta nahK$, we suspect HHQ can partially compensate for PQS binding and lead to similar phenotypic outcomes (33). Similar ideas have been shown for other PQS precursor and derivative molecules, including DHQ, which has been studied for its role in anaerobic respiration (50). In addition, PYO is thought to be used as an extracellular electron shuttle to promote anaerobic respiration in deep layers of biofilms that are not exposed to the environment (51, 52). It is possible that NO produced as a byproduct of anaerobic respiration is activating NosP signaling, which therefore inhibits NahK activity and, through modulating QS systems, produces more PYO to promote more anaerobic respiration. Because of this, it is possible NahK has not shown up in previous screens for phenazine regulators since its main role is specific to microaerobic conditions.

Overall, understanding how NahK links NO and QS may have important implications for how NO sensing controls molecular mechanisms in the bacteria. In infection, where immune cells secrete NO to combat bacterial invasion, it may be advantageous for NO to trigger cell density-independent PQS signaling through NosP inhibition of NahK (53). Indeed, one of the most intriguing results reported here is that $\Delta nahK$ turns on QS systems, or at least the PQS system, in a cell density-independent manner, which is consistent with this hypothesis. The PQS system drives activation of cytotoxicity through phenazine production, as well as activates iron acquisition systems and modulates host immune signaling (33). Therefore, NO signaling may be one early way bacteria activate counter-mechanisms to survive in a host because NosP responds to signaling levels of NO (6). Further characterization of the physiological relevance of NosP-mediated NO signaling during infection is necessary to understand how NO and QS integrate environmental signals.

MATERIALS AND METHODS

Bacterial strains, growth conditions, and media

The bacterial strains and plasmids used in this study are described in Tables S1 and S2. Oligonucleotides are described in Table S3. *P. aeruginosa* strains were grown aerobically in Luria-Bertani (LB) broth or succinate-based minimal media (35 mM K₂HPO₄, 22 mM KH₂PO₄, 7.6 mM (NH₄)Cl, 1.7 mM MgSO₄, 40 mM succinic acid, and 27.5 mM NaOH, pH 7.0) at 37°C (54). *Escherichia coli* strains were grown aerobically in LB broth or on LB agar at 37°C.

Generation of deletion strains

Markerless deletions were generated using methods previously described (8). In brief, 1 kb of flanking sequence for target locus was amplified and inserted in pMQ30 using gap repair cloning into *Saccharomyces cerevisiae* InvSc1. Plasmids were than transformed in *E. coli* donor strain WM3064 and conjugated into *P. aeruginosa* PA14 and selected for on LB agar plates containing 100 μ g/mL gentamicin. Double recombinants (markerless mutants) were then selected on a modified LB medium (containing 10% sucrose and lacking NaCl). Clones were confirmed via PCR.

Pyocyanin extraction

PYO extraction was performed as described previously elsewhere (55, 56). In brief, for planktonic culture, supernatant was collected from 100 mL succinate media cultures grown for 16–18 h. PYO was extracted via chloroform extraction, then extracted into 0.1M HCl for quantification. UV-visible light spectra was taken on a Varian Cary 100 Bio Spectrophotometer. PYO was quantified using Beer's law (extinction coefficient 17.072 μ g/mL) (55). For biofilm extraction, succinate-based minimal media agar plates (1% agar) were prepared using 35 mm \times 10 mm Petri dishes. Bacterial cultures were adjusted to an optical density (OD) of 0.8 before spotting onto agar plate. Biofilms were grown for 3 days at 25°C in the dark. The biofilm and agar were harvested and submerged in 4 mL of chloroform overnight 25°C in the dark. PYO was quantified as described above. For PYO quantification with exposure to M64 PqsR inhibitor, LB cultures at OD₆₀₀ of 0.05 were exposed to 1 μ M of M64 and grown for 16–18 h. PYO was extracted and quantified as described above.

C. elegans slow-killing assay

C. elegans slow-killing assay has been previously described as an effective method to observe *P. aeruginosa* virulence (51). One hundred microliters of PA14 wild type and PA14 Δ nahK were spotted onto slow-killing agar plates (0.3% NaCl, 0.35% Bacto-Peptone, 1 mM CaCl₂, 1 mM MgSO₄, 5 μ g/mL cholesterol, 25 mM KPO₄, 50 μ g/mL floxuridine

[FUDR], 1.7% agar). Plates were subsequently incubated 24 h at 37°C and then left for 48 h at room temperature. Thirty to thirty-five larval stage 4 *C. elegans* were transferred onto PA14 WT and PA14 Δ nahK seeded plates. Live worms were counted for 4 days.

Mung bean virulence assay

To assess the comparative virulence of PA14 $\Delta nahK$ to PA14 wild type, mung beans were exposed as described in Garge et al. with some minor modifications (57). Briefly, mung beans (Cool Beans N Sprouts) were washed in 70% (vol/vol) EtOH/water, a solution of 30% commercial bleach and 0.02% Triton X-100, and then rinsed three times with sterile ddH₂O. Sterilized mung beans were placed onto water agar (0.8%) and supplemented with 2 mL of sterilized ddH₂O and wrapped to maintain. Seeds were left to germinate for 24 h at 37°C. After germinating, sprouts of similar length and appearance were selected and randomly sorted into groups. Prepared overnight cultures of PA14 WT and PA14 $\Delta nahK$ were used to grow 100 mL cultures of each strain in fresh LB broth to an OD₆₀₀ of 1.0. The cultures were then centrifuged at 4,000 × g for 10 min and washed with 1X phosphate-buffered saline (PBS) once. Fresh PBS was added and cultures were adjusted to have the same OD₆₀₀. Then, 10 mL of the suspension was mixed in with the sprouts. All sprouts were covered in a suspension of bacteria, or PBS in the case of the control, and incubated at 30°C for 24 h.

After exposure to bacteria suspensions or PBS, each set of sprouts was rinsed with sterile ddH_2O . They were then transplanted to tubes with 30 mL of Murashige-Skoog agar. Each sprout was placed in a tube and covered with aluminum foil. After planting, plants were allowed to grow for 10 days. After 10 days, each plant was examined. Dead plants were identified by their lack of stalks and visible necrosis. After recording each plant's status, they were removed from the agar and the weight mass was recorded. Each plant was then placed on a glass sheet and scanned on an Epson Perfection V600 scanner. Each plant's longest root tendril and stalk length were recorded.

qPCR

PA14 wild type and $\Delta nahK$ were grown in 5 mL succinate media for 7 h at 37°C with agitation. Total cellular RNA from 5 mL cultures was isolated using the RNeasy Mini Kit (Qiagen). The yield and purity of the RNA was evaluated by Nanodrop and 1% agarose gel. cDNA was synthesized from 1 μ g of RNA using the RevertAid First Strand cDNA Synthesis Kit (Thermo Scientific). The 10 μ L qPCR reaction included 0.3 μ M of forward and reverse primer described in Table S1, equal amounts of cDNA, and 5 μ L of SYBR green master mix (Thermo Scientific). qPCR was performed on a Lightcycler 480. Cycling parameters were 95°C for 10 min, then 40 cycles of 95°C for 15 s and 60°C for 60 s. *GyrA* was used as a reference gene and relative expression was determined using a standard curve (58).

LCMS

Strains were grown for 24 h in 100 mL succinate media. Supernatant was collected by centrifugation, then twice filtered before LCMS was performed, as described for other bacteria elsewhere (59). LCMS was performed on a Bruker Impact II QTOF. The data were then compared to PAMDB database (http://pseudomonas.umaryland.edu) and the Bruker database (MetaboBASE), then analyzed using Metaboanalyst software (60).

Construction of reporter strains

Five hundred base pairs were amplified from the PA14 genome using primers listed in Table S3 and restriction cloned upstream of the coding sequence of *mScarlet* using Spel and Xhol digest sites in the multiple cloning site of pLD3208. Plasmids were verified by sequencing. Verified plasmids were introduced into *PA14* using biparental conjugation with *E. coli* S17-1. Single recombinants were selected on M9 minimal medium agar plates (47.8 mM Na₂HPO₄7H₂O, 2 mM KH₂PO₄, 8.6 mM NaCl, 18.6 mM NH₄Cl,

1 mM MgSO₄, 0.1 mM CaCl₂, 20 mM sodium citrate dihydrate, 1.5% agar) containing 70 μ g/mL gentamicin. The plasmid backbone was removed using flippase Flp-FRT recombination using the pFLP2 plasmid (61) and selection on M9 minimal medium agar plates containing 300 μ g/mL carbenicillin. pFLP2 plasmid was cured by streaking on LB agar plates without NaCl with 10% wt/vol sucrose. The presence of *mScarlet* in final clones was confirmed by PCR.

Transcriptional mScarlet fluorescence assays

For reporter assays, strains containing mScarlet *phz1* or *phz2* reporters were grown overnight in 5 mL LB, then 1:100 diluted into black walled, clear bottom 96-well plates containing 200 µL succinate media. Over 24 h, every 30 min, the fluorescence (e.g., 560 nm–610 nm) and optical density at 600 nm was determined for every well on a SpectraMax iD3 plate reader. For mixing assays, strains were mixed together in a 1:1 ratio of fluorescent, mScarlet-expressing and non-fluorescent cells. Over 24 h, every 30 min, the fluorescence (e.g., 560 nm–610 nm) and optical density at 600 nm was determined for every well on a SpectraMax iD3 plate reader (8). Plates were continuously shaking and incubated at 37°C.

AUTHOR AFFILIATIONS

¹Department of Microbiology and Immunology, Stony Brook University, Stony Brook, New York, USA

²Department of Molecular and Cellular Biology, Stony Brook University, Stony Brook, New York, USA

³Department of Biological Sciences, Columbia University, New York, New York, USA

AUTHOR ORCIDs

Alicia G. Mendoza http://orcid.org/0000-0001-5010-2951 Lars E. P. Dietrich http://orcid.org/0000-0003-2049-1137 Elizabeth M. Boon http://orcid.org/0000-0003-1891-839X

FUNDING

Funder	Grant(s)	Author(s)
HHS National Institutes of Health (NIH)	GM118894	Elizabeth M. Boon
HHS National Institutes of Health (NIH)	T32GM136572	Elizabeth M. Boon

AUTHOR CONTRIBUTIONS

Alicia G. Mendoza, Conceptualization, Data curation, Formal analysis, Investigation, Methodology, Validation, Visualization, Writing – original draft, Writing – review and editing | Danielle Guercio, Data curation, Formal analysis, Investigation, Methodology, Visualization, Writing – original draft, Writing – review and editing | Marina K. Smiley, Investigation, Methodology, Writing – review and editing | Gaurav K. Sharma, Investigation | Jason M. Withorn, Investigation, Methodology | Natalie V. Hudson-Smith, Investigation, Methodology | Chika Ndukwe, Investigation | Lars E. P. Dietrich, Conceptualization, Methodology, Supervision, Writing – review and editing | Elizabeth M. Boon, Conceptualization, Formal analysis, Funding acquisition, Methodology, Project administration, Resources, Software, Supervision, Writing – original draft, Writing – review and editing

ADDITIONAL FILES

The following material is available online.

⁴Department of Chemistry, Stony Brook University, Stony Brook, New York, USA

Supplemental Material

Supplemental material (JB00276-23-s0001.pdf). Tables S1 to S4 and Fig. S1 to S6.

REFERENCES

- Qin S, Xiao W, Zhou C, Pu Q, Deng X, Lan L, Liang H, Song X, Wu M. 2022. Pseudomonas aeruginosa: pathogenesis, virulence factors, antibiotic resistance, interaction with host, technology advances and emerging therapeutics. Signal Transduct Target Ther 7:199. https://doi.org/10. 1038/s41392-022-01056-1
- Maes M, Higginson E, Pereira-Dias J, Curran MD, Parmar S, Khokhar F, Cuchet-Lourenço D, Lux J, Sharma-Hajela S, Ravenhill B, Hamed I, Heales L, Mahroof R, Soderholm A, Forrest S, Sridhar S, Brown NM, Baker S, Navapurkar V, Dougan G, Scott JB, Morris AC. 2021. Correction to: ventilator-associated pneumonia in critically ill patients with COVID-19. Crit Care 25:130. https://doi.org/10.1186/s13054-021-03560-2
- Francis VI, Porter SL. 2019. Multikinase networks: two-component signaling networks integrating multiple stimuli. Annu Rev Microbiol 73:199–223. https://doi.org/10.1146/annurev-micro-020518-115846
- Tumbarello M, De Pascale G, Trecarichi EM, Spanu T, Antonicelli F, Maviglia R, Pennisi MA, Bello G, Antonelli M. 2013. Clinical outcomes of Pseudomonas aeruginosa pneumonia in intensive care unit patients. Intensive Care Med 39:682–692. https://doi.org/10.1007/s00134-013-2828-9
- Song H, Li Y, Wang Y. 2023. Two-component system GacS/GacA, a global response regulator of bacterial physiological behaviors. Eng Microbiol 3:100051. https://doi.org/10.1016/j.engmic.2022.100051
- Hossain S, Boon EM. 2017. Discovery of a novel nitric oxide binding protein and nitric-oxide-responsive signaling pathway in *Pseudomonas* aeruginosa. ACS Infect Dis 3:454–461. https://doi.org/10.1021/ acsinfecdis.7b00027
- Kong W, Chen L, Zhao J, Shen T, Surette MG, Shen L, Duan K. 2013. Hybrid sensor kinase PA1611 in *Pseudomonas aeruginosa* regulates transitions between acute and chronic infection through direct interaction with RetS. Mol Microbiol 88:784–797. https://doi.org/10. 1111/mmi.12223
- Wang BX, Wheeler KM, Cady KC, Lehoux S, Cummings RD, Laub MT, Ribbeck K. 2021. Mucin glycans signal through the sensor kinase RetS to inhibit virulence-associated traits in *Pseudomonas aeruginosa*. Curr Biol 31:90–102. https://doi.org/10.1016/j.cub.2020.09.088
- Price-Whelan A, Dietrich LEP, Newman DK. 2006. Rethinking "secondary" metabolism: physiological roles for phenazine antibiotics. Nat Chem Biol 2:71–78. https://doi.org/10.1038/nchembio764
- Anantharaman S, Guercio D, Mendoza AG, Withorn JM, Boon EM. 2023.
 Negative regulation of biofilm formation by nitric oxide sensing proteins. Biochem Soc Trans 51:1447–1458. https://doi.org/10.1042/ BST20220845
- Hsu J-L, Chen H-C, Peng H-L, Chang H-Y. 2008. Characterization of the histidine-containing phosphotransfer protein B-mediated multistep phosphorelay system in *Pseudomonas aeruginosa* PAO1. J Biol Chem 283:9933–9944. https://doi.org/10.1074/jbc.M708836200
- Thöming JG, Tomasch J, Preusse M, Koska M, Grahl N, Pohl S, Willger SD, Kaever V, Müsken M, Häussler S. 2020. Parallel evolutionary paths to produce more than one *Pseudomonas aeruginosa* biofilm phenotype. NPJ Biofilms Microbiomes 6:2. https://doi.org/10.1038/s41522-019-0113-6
- Lee J, Zhang L. 2015. The hierarchy quorum sensing network in Pseudomonas aeruginosa. Protein Cell 6:26–41. https://doi.org/10.1007/ s13238-014-0100-x
- Recinos DA, Sekedat MD, Hernandez A, Cohen TS, Sakhtah H, Prince AS, Price-Whelan A, Dietrich LEP. 2012. Redundant phenazine operons in Pseudomonas aeruginosa exhibit environment-dependent expression and differential roles in pathogenicity. Proc Natl Acad Sci U S A 109:19420–19425. https://doi.org/10.1073/pnas.1213901109
- Higgins S, Heeb S, Rampioni G, Fletcher MP, Williams P, Cámara M. 2018.
 Differential regulation of the phenazine biosynthetic operons by quorum sensing in *Pseudomonas aeruginosa* PAO1-N. Front Cell Infect Microbiol 8:252. https://doi.org/10.3389/fcimb.2018.00252
- Sakhtah H, Koyama L, Zhang Y, Morales DK, Fields BL, Price-Whelan A, Hogan DA, Shepard K, Dietrich LEP. 2016. The Pseudomonas aeruginosa

- efflux pump MexGHI-OpmD transports a natural phenazine that controls gene expression and biofilm development. Proc Natl Acad Sci U S A 113:E3538–E3547. https://doi.org/10.1073/pnas.1600424113
- Park S, Sauer K. 2021. SagS and its unorthodox contributions to Pseudomonas aeruginosa biofilm development. Biofilm 3:100059. https://doi.org/10.1016/j.bioflm.2021.100059
- Kay E, Humair B, Dénervaud V, Riedel K, Spahr S, Eberl L, Valverde C, Haas D. 2006. Two GacA-dependent small RNAs modulate the quorumsensing response in *Pseudomonas aeruginosa*. J Bacteriol 188:6026– 6033. https://doi.org/10.1128/JB.00409-06
- Jean-Pierre F, Tremblay J, Déziel E. 2016. Broth versus surface-grown cells: differential regulation of RsmY/Z small RNAs in *Pseudomonas* aeruginosa by the GAC/HptB system. Front Microbiol 7:2168. https://doi. org/10.3389/fmicb.2016.02168
- Rahme LG, Stevens EJ, Wolfort SF, Shao J, Tompkins RG, Ausubel FM. 1995. Common virulence factors for bacterial pathogenicity in plants and animals. Science 268:1899–1902. https://doi.org/10.1126/science. 7604262
- Essar DW, Eberly L, Hadero A, Crawford IP. 1990. Identification and characterization of genes for a second anthranilate synthase in *Pseudomonas aeruginosa*: interchangeability of the two anthranilate synthases and evolutionary implications. J Bacteriol 172:884–900. https://doi.org/10.1128/jb.172.2.884-900.1990
- Hall S, McDermott C, Anoopkumar-Dukie S, McFarland AJ, Forbes A, Perkins AV, Davey AK, Chess-Williams R, Kiefel MJ, Arora D, Grant GD. 2016. Cellular effects of pyocyanin, a secreted virulence factor of Pseudomonas aeruginosa. Toxins (Basel) 8:236. https://doi.org/10.3390/ toxins8080236
- Mavrodi DV, Bonsall RF, Delaney SM, Soule MJ, Phillips G, Thomashow LS. 2001. Functional analysis of genes for biosynthesis of pyocyanin and phenazine-1-carboxamide from *Pseudomonas aeruginosa* PAO1. J Bacteriol 183:6454–6465. https://doi.org/10.1128/JB.183.21.6454-6465. 2001
- Parsons JF, Greenhagen BT, Shi K, Calabrese K, Robinson H, Ladner JE. 2007. Structural and functional analysis of the pyocyanin biosynthetic protein PhzM from *Pseudomonas aeruginosa*. Biochemistry 46:1821– 1828. https://doi.org/10.1021/bi6024403
- Greenhagen BT, Shi K, Robinson H, Gamage S, Bera AK, Ladner JE, Parsons JF. 2008. Crystal structure of the pyocyanin biosynthetic protein PhzS. Biochemistry 47:5281–5289. https://doi.org/10.1021/bi702480t
- Huang J, Xu Y, Zhang H, Li Y, Huang X, Ren B, Zhang X. 2009. Temperature-dependent expression of *phzM* and its regulatory genes *lasl* and *ptsP* in rhizosphere isolate *Pseudomonas* sp. strain M18. Appl Environ Microbiol 75:6568–6580. https://doi.org/10.1128/AEM.01148-09
- Huang J, Sonnleitner E, Ren B, Xu Y, Haas D. 2012. Catabolite repression control of pyocyanin biosynthesis at an intersection of primary and secondary metabolism in *Pseudomonas aeruginosa*. Appl Environ Microbiol 78:5016–5020. https://doi.org/10.1128/AEM.00026-12
- Mavrodi DV, Blankenfeldt W, Thomashow LS. 2006. Phenazine compounds in fluorescent *Pseudomonas* spp. biosynthesis and regulation. Annu Rev Phytopathol 44:417–445. https://doi.org/10.1146/ annurev.phyto.44.013106.145710
- Mavrodi DV, Peever TL, Mavrodi OV, Parejko JA, Raaijmakers JM, Lemanceau P, Mazurier S, Heide L, Blankenfeldt W, Weller DM, Thomashow LS. 2010. Diversity and evolution of the phenazine biosynthesis pathway. Appl Environ Microbiol 76:866–879. https://doi. org/10.1128/AEM.02009-09
- Schuster M, Urbanowski ML, Greenberg EP. 2004. Promoter specificity in Pseudomonas aeruginosa quorum sensing revealed by DNA binding of purified LasR. Proc Natl Acad Sci U S A 101:15833–15839. https://doi.org/ 10.1073/pnas.0407229101
- Whiteley M, Lee KM, Greenberg EP. 1999. Identification of genes controlled by quorum sensing in *Pseudomonas aeruginosa*. Proc Natl Acad Sci U S A 96:13904–13909. https://doi.org/10.1073/pnas.96.24. 13904

- 32. Rampioni G, Bertani I, Zennaro E, Polticelli F, Venturi V, Leoni L. 2006. The quorum-sensing negative regulator RsaL of *Pseudomonas aeruginosa* binds to the lasl promoter. J Bacteriol 188:815–819. https://doi.org/10.1128/JB.188.2.815-819.2006
- Lin J, Cheng J, Wang Y, Shen X. 2018. The *Pseudomonas* quinolone signal (PQS): not just for quorum sensing anymore. Front Cell Infect Microbiol 8:230. https://doi.org/10.3389/fcimb.2018.00230
- Déziel E, Lépine F, Milot S, He J, Mindrinos MN, Tompkins RG, Rahme LG. 2004. Analysis of *Pseudomonas aeruginosa* 4-hydroxy-2-alkylquinolines (HAQs) reveals a role for 4-hydroxy-2-heptylquinoline in cell-to-cell communication. Proc Natl Acad Sci U S A 101:1339–1344. https://doi. org/10.1073/pnas.0307694100
- Mukherjee S, Moustafa DA, Stergioula V, Smith CD, Goldberg JB, Bassler BL. 2018. The PqsE and RhIR proteins are an autoinducer synthase– receptor pair that control virulence and biofilm development in Pseudomonas aeruginosa. Proc Natl Acad Sci U S A 115:E9411–E9418. https://doi.org/10.1073/pnas.1814023115
- Wang Y, Gao L, Rao X, Wang J, Yu H, Jiang J, Zhou W, Wang J, Xiao Y, Li M, Zhang Y, Zhang K, Shen L, Hua Z. 2018. Characterization of lasR-deficient clinical isolates of *Pseudomonas aeruginosa*. Sci Rep 8:13344. https://doi. org/10.1038/s41598-018-30813-y
- Balasubramanian D, Schneper L, Kumari H, Mathee K. 2013. A dynamic and intricate regulatory network determines *Pseudomonas aeruginosa* virulence. Nucleic Acids Res 41:1–20. https://doi.org/10.1093/nar/ qks1039
- Ha C, Park SJ, Im S-J, Park S-J, Lee J-H. 2012. Interspecies signaling through QscR, a quorum receptor of *Pseudomonas aeruginosa*. Mol Cells 33:53–59. https://doi.org/10.1007/s10059-012-2208-2
- Siehnel R, Traxler B, An DD, Parsek MR, Schaefer AL, Singh PK. 2010. A unique regulator controls the activation threshold of quorum-regulated genes in *Pseudomonas aeruginosa*. Proc Natl Acad Sci U S A 107:7916– 7921. https://doi.org/10.1073/pnas.0908511107
- Seet Q, Zhang L-H. 2011. Anti-activator QsIA defines the quorum sensing threshold and response in *Pseudomonas aeruginosa*. Mol Microbiol 80:951–965. https://doi.org/10.1111/j.1365-2958.2011.07622.x
- 41. Wang T, Sun W, Fan L, Hua C, Wu N, Fan S, Zhang J, Deng X, Yan J. 2021. An atlas of the binding specificities of transcription factors in *Pseudomonas aeruginosa* directs prediction of novel regulators in virulence. Elife 10:e61885. https://doi.org/10.7554/eLife.61885
- Starkey M, Lepine F, Maura D, Bandyopadhaya A, Lesic B, He J, Kitao T, Righi V, Milot S, Tzika A, Rahme L. 2014. Identification of anti-virulence compounds that disrupt quorum-sensing regulated acute and persistent pathogenicity. PLoS Pathog 10:e1004321. https://doi.org/10.1371/ journal.ppat.1004321
- Hossain S, Heckler I, Boon EM. 2018. Discovery of a nitric oxide responsive quorum sensing circuit in *Vibrio cholerae*. ACS Chem Biol 13:1964–1969. https://doi.org/10.1021/acschembio.8b00360
- Williams DE, Boon EM. 2019. Towards understanding the molecular basis of nitric oxide-regulated group behaviors in pathogenic bacteria. J Innate Immun 11:205–215. https://doi.org/10.1159/000494740
- Heckler I, Boon EM. 2019. Insights into nitric oxide modulated quorum sensing pathways. Front Microbiol 10:2174. https://doi.org/10.3389/ fmicb.2019.02174
- Pessi G, Williams F, Hindle Z, Heurlier K, Holden MT, Cámara M, Haas D, Williams P. 2001. The global posttranscriptional regulator RsmA modulates production of virulence determinants and N-acylhomoserine lactones in *Pseudomonas aeruginosa*. J Bacteriol 183:6676–6683. https:// doi.org/10.1128/JB.183.22.6676-6683.2001

- Nisbett L-M, Binnenkade L, Bacon B, Hossain S, Kotloski NJ, Brutinel ED, Hartmann R, Drescher K, Arora DP, Muralidharan S, Thormann KM, Gralnick JA, Boon EM. 2019. Nosp signaling modulates the NO/H-NOXmediated multicomponent C-Di-GMP network and biofilm formation in Shewanella oneidensis. Biochemistry 58:4827–4841. https://doi.org/10. 1021/acs.biochem.9b00706
- Letizia M, Mellini M, Fortuna A, Visca P, Imperi F, Leoni L, Rampioni G. 2022. PqsE expands and differentially modulates the RhIR quorum sensing regulon in *Pseudomonas aeruginosa*. Microbiol Spectr 10:e0096122. https://doi.org/10.1128/spectrum.00961-22
- Arai H. 2011. Regulation and function of versatile aerobic and anaerobic respiratory metabolism in *Pseudomonas aeruginosa*. Front Microbiol 2:103. https://doi.org/10.3389/fmicb.2011.00103
- Gruber JD, Chen W, Parnham S, Beauchesne K, Moeller P, Flume PA, Zhang Y-M. 2016. The role of 2,4-dihydroxyquinoline (DHQ) in Pseudomonas aeruginosa pathogenicity. PeerJ 4:e1495. https://doi.org/ 10.7717/peerj.1495
- 51. Jo J, Cortez KL, Cornell WC, Price-Whelan A, Dietrich LE. 2017. An orphan cbb3-type cytochrome oxidase subunit supports *Pseudomonas aeruginosa* biofilm growth and virulence. eLife 6:e30205.
- Dietrich LEP, Okegbe C, Price-Whelan A, Sakhtah H, Hunter RC, Newman DK. 2013. Bacterial community morphogenesis is intimately linked to the intracellular redox state. J Bacteriol 195:1371–1380. https://doi.org/ 10.1128/JB.02273-12
- Schairer DO, Chouake JS, Nosanchuk JD, Friedman AJ. 2012. The potential of nitric oxide releasing therapies as antimicrobial agents. Virulence 3:271–279. https://doi.org/10.4161/viru.20328
- Hoegy F, Mislin GLA, Schalk IJ. 2014. Pyoverdine and pyochelin measurements. Methods Mol Biol 1149:293–301. https://doi.org/10. 1007/978-1-4939-0473-0_24
- Muller M, Merrett ND. 2014. Pyocyanin production by *Pseudomonas aeruginosa* confers resistance to ionic silver. Antimicrob Agents Chemother 58:5492–5499. https://doi.org/10.1128/AAC.03069-14
- Dietrich LEP, Price-Whelan A, Petersen A, Whiteley M, Newman DK. 2006.
 The phenazine pyocyanin is a terminal signalling factor in the quorum sensing network of *Pseudomonas aeruginosa*. Mol Microbiol 61:1308–1321. https://doi.org/10.1111/j.1365-2958.2006.05306.x
- Garge S, Azimi S, Diggle SP. 2018. A simple mung bean infection model for studying the virulence of *Pseudomonas aeruginosa*. Microbiology (Reading) 164:764–768. https://doi.org/10.1099/mic.0.000659
- Alqarni B, Colley B, Klebensberger J, McDougald D, Rice SA. 2016. Expression stability of 13 housekeeping genes during carbon starvation of *Pseudomonas aeruginosa*. J Microbiol Methods 127:182–187. https:// doi.org/10.1016/j.mimet.2016.06.008
- Nandakumar M, Prosser GA, de Carvalho LPS, Rhee K. 2015. Metabolomics of Mycobacterium tuberculosis. Methods Mol Biol 1285:105–115. https://doi.org/10.1007/978-1-4939-2450-9_6
- Pang Z, Zhou G, Ewald J, Chang L, Hacariz O, Basu N, Xia J. 2022. Using MetaboAnalyst 5.0 for LC–HRMS spectra processing, multi-omics integration and covariate adjustment of global metabolomics data. Nat Protoc 17:1735–1761. https://doi.org/10.1038/s41596-022-00710-w
- Hoang TT, Karkhoff-Schweizer RR, Kutchma AJ, Schweizer HP. 1998. A broad-host-range FLP-FRT recombination system for site-specific excision of chromosomally-located DNA sequences: application for isolation of unmarked *Pseudomonas aeruginosa* Mutants. Gene 212:77– 86. https://doi.org/10.1016/s0378-1119(98)00130-9